Available online at www.sciencedirect.com
SCIENCE DIRECT®
Journal of Solid State Chemistry 179 (2006) 2674–2680
JOURNAL OF SOLID STATE CHEMISTRY
www.elsevier.com/locate/jssc

# Supercritical Propanol–Water Synthesis and Comprehensive Size Characterisation of Highly Crystalline anatase $TiO_2$ Nanoparticles

Peter Hald[a], Jacob Becker[a], Martin Bremholm[a], Jan S. Pedersen[a], Jacques Chevallier[b], Steen B. Iversen[c], Bo B. Iversen[a,*]

[a]*Department of Chemistry, University of Aarhus, DK-8000 Aarhus, Denmark*
[b]*Department of Physics, University of Aarhus, DK-8000 Aarhus, Denmark*
[c]*SCF Technologies, Gl. Køgelandevej 22, DK-2500 Valby, Denmark*

Received 21 December 2005; received in revised form 3 May 2006; accepted 4 May 2006
Available online 23 May 2006

**Abstract**

Highly crystalline anatase $TiO_2$ nanoparticles have been synthesised in less than 1 min in a supercritical propanol–water mixture using a continuous flow reactor. The synthesis parameter space ($T$, $P$, concentration) has been explored and the average particle size can be accurately controlled within 10–18 nm with narrow size distributions (2–3 nm). At subcritical conditions amorphous products are obtained, whereas a broad range of $T$ and $P$ in the supercritical regime gives 11–14 nm particles. At high temperature and pressure, the particles size increase to 18 nm. The nanoparticles have been extensively characterised with powder X-ray diffraction (PXRD), transmission electron microscopy (TEM) and small-angle X-ray scattering (SAXS) with excellent agreement on size and size distribution parameters. The SAXS analysis suggests disk-shaped particles with diameters that are approximately double the height. For comparison, a series of conventional autoclave sol–gel syntheses have been carried out. These also produce phase-pure anatase nanoparticles, but with much broader size distributions and at much longer synthesis times (hours). The study demonstrates that synthesis in supercritical fluids is a very promising method for manipulating the size and size distribution of nanoparticles, thus removing one of the key limitations in many applications of nanomaterials.


*Keywords:* Supercritical fluids; Nanoparticles; Size and size distributions; Oxides

## 1. Introduction

Nanomaterials are cornerstones in many attempts to develop and exploit nanotechnology. During the last decades, the insight into structures of nanomaterials has dramatically improved through application of new and improved methods for characterisation [1]. However, in applications of nanomaterials it is often the primary synthesis, which is limiting further exploitation. It is therefore important to focus on new processing technologies if nanomaterials are to become competitive in the market. One critical issue is that in order to have well-defined size-dependent properties, it is essential to have a narrow size distribution of the material.

Numerous techniques are being developed for producing nanopowders including high-temperature gas synthesis methods such as flame synthesis and plasma arc processes [2]. Solution sol–gel, solvothermal (including hydrothermal), and microemulsion techniques are the major low-temperature processes for synthesis of nanomaterials [2]. Sol–gel processing is widely used as it is a versatile technology to produce high-purity materials with a relative small particle size. The key drawbacks of the sol–gel process are that it is time consuming, and the materials need post-treatment such as drying and calcination. In addition to a higher energy usage and a more complicated process, this has the unfortunate effect of crystal growth. One problem with conventional solvothermal batch methods is the quite uncontrolled temperature and pressure as well as slow process time, which leads to broad size distributions of the particles. Microemulsion techniques

*Corresponding author. Fax: +43 86 19 61 99.
*E-mail address:* bo@chem.au.dk (B.B. Iversen).

0022-4596/$ - see front matter © 2006 Elsevier Inc. All rights reserved.
doi:10.1016/j.jssc.2006.05.012

give highly homogenous particles (i.e., narrow size distributions), but it is a relatively slow batch process with limited chemical flexibility.

Another approach to synthesis of nanoparticles is to use supercritical fluids [3]. Supercritical fluids exhibit particularly attractive properties such as gas-like transport properties (diffusivity, viscosity and surface tension), yet they also have liquid-like properties such as high-solvation capability and density. Furthermore, the solubility can be effectively manipulated by small changes in pressure and temperature. This tuneable solubility is a unique property that makes supercritical fluids different from conventional solvents. The properties of supercritical fluids have attracted attention, e.g., for potential applications as environmentally friendly solvents for chemical processing [4]. Carbon dioxide is the most widely used fluid for dense fluid applications because of its moderate critical constants, non-toxic nature, low cost and availability in pure form. Supercritical $CO_2$ is typically applied commercially in extraction processes such as decaffeination of coffee, but many other applications of supercritical fluids have been reported including synthesis of submicron-sized particles [5].

Here we report on synthesis of highly homogenous anatase $TiO_2$ nanoparticles using a continuous-flow supercritical system that allows quick exploration of synthesis parameter space (temperature, pressure, concentration). For comparison, a conventional sol–gel process has also been explored. The particles have been extensively characterised using powder X-ray diffraction (PXRD), transmission electron microscopy (TEM) and small-angle X-ray scattering (SAXS). Especially, the latter technique is relatively rare in the literature on supercritical nanoparticle synthesis. This is unfortunate since comparison of SAXS results with more conventional TEM and PXRD results allow conclusions about crystallinity of the particles to be made. The crystallinity of the synthesised particles is highly important in many applications, since it strongly affects the physical and chemical properties of the sample. Our synthesis system has large chemical flexibility, and unlike batch systems there is no operating downtime [6]. We have synthesised the $TiO_2$ nanoparticles with a narrow size distribution using titaniumisopropoxide in a mixture of supercritical isopropanol and water (5%). Synthesis in supercritical 2-propanol without addition of water gives no reaction. There has been intense interest in nanosized $TiO_2$ both in basic science and in industry due to a range of unique properties (e.g., photocatalysis, solar cells) [7]. The synthesis times in our apparatus are short (seconds) since we mix the extremely hot supercritical solvent with the cold reactant. Besides giving control over temperature and pressure, this leads to instantaneous crystallisation, where crystal nucleation far exceeds crystal growth. In most other synthesis methods there are process steps, where the mass or heat is poorly controlled. The removal of such process steps is what leads to narrow particle size distributions in the supercritical method.

## 2. Experimental

### 2.1. Synthesis

The supercritical synthesis system we use is sketched in Fig. 1. The essential features are that all pumps are kept "cold", and that the synthesis is continuous, which allows scaling and complete control over synthesis parameters. The only expensive material required is for the pipes and the reactor block, which are made out of the highly corrosion-resistant alloy Inconel625. In our setup, the solvent is first pressurised and then pumped into a standard tube furnace using standard air-driven liquid pumps. After reaching the desired temperature and pressure, the (supercritical) solvent meets one or more reactant solution(s) in the reactor block, and the reaction then takes place immediately upon mixing as well as during the backflow through the furnace. The superheating of the solvent string relative to the reactant string can be maintained all the way through the reactor block, which is temperature controlled by resistance heaters drilled into the block. Once outside the furnace, effective cooling of the reaction mixture is performed to save pressure and product outlets. All "cold" components are made of standard Steel 316, which can handle up to 1500 bar and 150 °C.

As a reference experiment we have synthesised $TiO_2$ by the sol–gel method of Kolen'ko et al. [8]; 100 mL $TiCl_4$ was slowly added to 750 mL water and crushed ice. Additional ice was added as it melted, and this resulted in a clear but very acidic yellow solution. $TiO_2$-gel was precipitated by adding concentrated ammonia solution up to pH = 8, and the gel was washed chloride free by repeated centrifugation and redispersion in water. This resulted in a white gel with a water content of 85%. The gel was transferred to 15 mL autoclaves, which were filled 2/3 with the gel and heated to 150, 200 and 250 °C, respectively. Furthermore, the synthesis time was varied between $^1/_2$, 1, $1^1/_2$, 2 and 24 h for each temperature producing a total of 15 synthesis products.

### 2.2. Powder X-ray diffraction

PXRD data were measured on a STOE powder diffractometer at the Department of Chemistry, University of Aarhus, Denmark. A Ge(1 1 1) single crystal monochromator

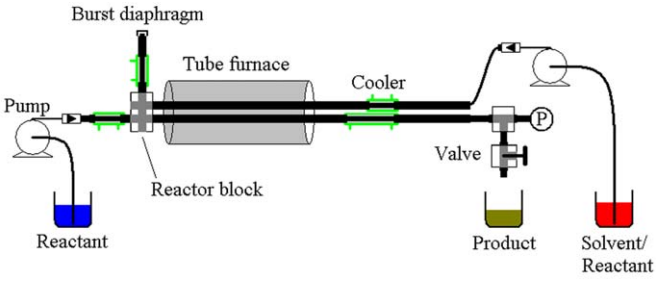


Fig. 1. Sketch of the supercritical synthesis equipment.

was used to produce Cu$K_{\alpha 1}$ radiation, which was detected with a 40° position sensitive detector. The Scherrer equation gives the volume weighted particle size as $D = 0.94 \times 0.154\,\text{nm}/(\text{FWHM*cos }\theta)$ in the Gaussian approximation for Cu$K_\alpha$ radiation. The full-width at half maximum of the peak (FWHM) is in radians. The instrumental broadening was obtained from the peak width of a $LaB_6$ standard sample. For all samples, the (101) peak was fitted with a Pseudo-Voigt function, and the Gaussian component was in all cases between 50% and 70%. In a Gaussian model for the peak widths, the total width is given as $W^2_{\text{total}} = W^2_{\text{particle}} + W^2_{\text{inst}}$, whereas a purely Lorentzian peak width gives $W_{\text{total}} = W_{\text{particle}} + W_{\text{inst}}$. These two estimates bracket the actual peak width, and provides lower and upper estimates of the particle size. For further description of standard powder diffraction methods to obtain particle sizes, please see the seminal books by Warren [9] or by Guinier [10].

### 2.3. Small angle X-ray scattering

The SAXS measurements were performed on a Bruker AXS Nanostar pin-hole camera optimized for solution scattering at the Department of Chemistry, University of Aarhus, Denmark [11]. Suspensions of the nanoparticles were prepared with the concentrations less than 1 wt%. The suspensions were flame sealed in boron silicate capillaries, which were placed directly in the vacuum of the SAXS instrument. A capillary filled with solvent was measured and subtracted as background from the sample measurements. The azimuthally averaged data were least-squares fitted using a model of polydisperse particles [12]. The data were fitted using form factors of flat disks with diameter $D$ and height $H$, and a Schultz size distribution [13]. The size variation between particles was assumed to be affine, so that only one distribution had to be included.

### 2.4. Transmission electron microscopy

TEM images were recorded on a Philips CM20 working at 200 kV at the Department of Physics, University of Aarhus, Denmark. A drop of the particle suspensions was deposited on a carbon-coated TEM grid and allowed to dry before investigation.

## 3. Results and discussion

### 3.1. Supercritical synthesis

First we show results for a synthesis run, where temperature and pressure was changed continuously for constant reactant concentration and no heating on the reaction block, Table 1. The supercritical solvent was 2-propanol ($T_c = 235.6\,^\circ\text{C}$, $P_c = 53.7$ bar) with 5% water and the reactant solution was 0.1 M titaniumisopropoxide (ACROS 98%) in 2-propanol. The experiment used a flow rate of approximately 20 mL/min.

Determination of particle sizes and size distributions is a key issue in all research focussed on nanopowders [14], and here we establish these parameters not only by PXRD and TEM, but also by SAXS. The results obtained with the three different methods agree very well. From the PXRD data, we can qualitatively monitor the crystallinity of the product, Fig. 2, and based on the peak width the volume averaged particle size was estimated using the Scherrer equation [15]. Use of a low-order reflection in the size estimate minimises the effect of strain broadening. The Scherrer estimate is a lower estimate of the particle size, and as seen in Table 1 it ranges from 11–18 nm for the different crystalline products. For all synthesis runs above the critical point, single-phase anatase is obtained. The particle size estimates obtained from the SAXS data are in very good agreement with the PXRD estimates, Table 1.

Table 1
Experimental details for the 13 synthesis products obtained with variable temperature and pressure

| Product | Pressure (bar) | $T_{\text{pipe}}$ (°C) | $T_{\text{block}}$ (°C) | $D_{\text{SAXS}}$ (nm) | $H_{\text{SAXS}}$ (nm) | $D_{\text{PXRD}}$ (nm) |
|---|---|---|---|---|---|---|
| 1 | 58 | 137 | 75 | Gel | | Amorphous |
| 2 | 160 | 142 | 75 | Gel | | Amorphous |
| 3 | 300 | 145 | 80 | Gel | | Amorphous |
| 4 | 450 | 139 | 84 | Gel | | Amorphous |
| 5 | 58 | 238 | 110 | 11.5 | 4.9 | 12.0 (15.7) |
| 6 | 150 | 239 | 118 | 10.7 | 5.4 | 11.7 (15.3) |
| 7 | 300 | 233 | 125 | 10.7 | 4.4 | 10.6 (13.4) |
| 8 | 450 | 235 | 132 | 11.2 | 4.7 | 11.4 (14.7) |
| 9 | 58 | 295 | 150 | 11.5 | 4.8 | 12.8 (16.9) |
| 10 | 150 | 305 | 155 | 13.5 | 4.5 | 12.8 (16.9) |
| 11 | 300 | 318 | 165 | 11.7 | 5.1 | 11.3 (14.5) |
| 12 | 460 | 308 | 175 | 16.3 | 5.3 | 13.9 (18.9) |
| 13 | 500 | 430 | 245 | 17.1 | 7.5 | 17.2 (25.0) |

For SAXS, $D$ is the diameter, and $H$ the height of the flat disk model used to fit the data [13]. For the SAXS fits, the relative polydispersity was between 0.39 and 0.47 [13]. For PXRD, $D$ is the volume-averaged diameter of the particles corrected for instrumental broadening using a Gaussian model for the peak widths $W$ ($W^2_{\text{total}} = W^2_{\text{particle}} + W^2_{\text{inst}}$) [9,10]. In parenthesis values obtained with a Lorentzian correction are listed ($W_{\text{total}} = W_{\text{particle}} + W_{\text{inst}}$).

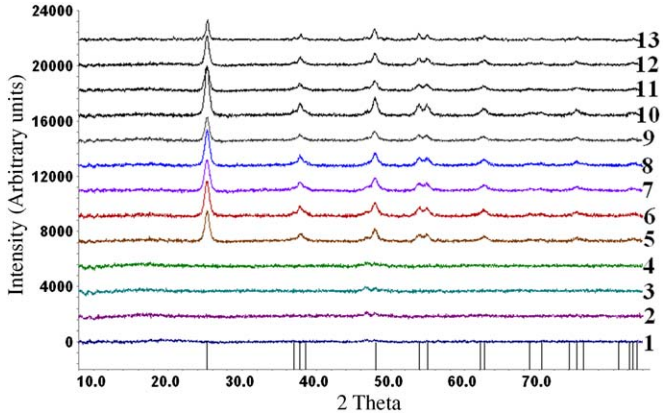


Fig. 2. Powder X-ray diffraction data of the supercritical synthesis products in Table 1. The vertical bars correspond to the diffraction angles of anatase.

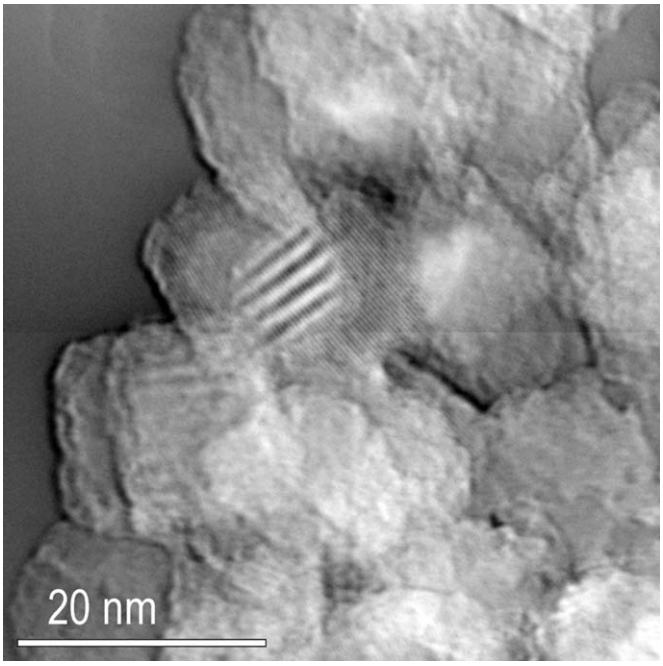


Fig. 3. HRTEM of supercritical synthesis product 11 showing crystal lattices extending to the edges of the crystallites. A Moire pattern is seen where two crystallites overlap.

Typically the diameter of the disk-shaped particles is within 1 nm of the PXRD crystallite size estimate. On the other hand, the height of the disk is only half the diameter suggesting anisotropic particles. This is somewhat at variance with the PXRD data, where the peak widths only have a slight increase with scattering angle. A Williamson–Hall type plot therefore indicates limited strain as well as limited size anisotropy. Nevertheless, the agreement between SAXS *particle* size estimates, and PXRD *crystallite* size estimates suggests that the particles are highly crystalline. This is also supported by HRTEM images, which reveal that the crystal lattices extend to the edges of the crystallites, Fig. 3.

The TEM image, Fig. 4a, is illustrative of the high homogeneities of the samples, and all particles appear of equal size. The estimate of the size distribution from TEM is also shown in Fig. 4a. Indeed the particles have a very narrow size distribution ($13 \pm 2$ nm), and the average size is in excellent agreement with the PXRD and SAXS result. This demonstrates that the grains observed in the TEM images in fact are the individual nanoparticles. For comparison the conventional sol–gel synthesis technique gives larger particles with a much broader size distribution ($22 \pm 8$ nm), Fig. 4b. Size distributions can also be estimated from the SAXS data, and in Fig. 5 we have plotted distributions for products 8, 11 and 13. The SAXS data indicate slightly broader distributions than estimated from the TEM images. Overall, the data in Table 1 reveal that under subcritical conditions no crystalline particles are formed (products 1-4). In the supercritical state, there is a quite broad region in temperature and pressure, where the products have similar sizes (11–12 nm). At very high pressure and temperature, there is an increase in particle size to 18 nm.

In a second synthesis run we vary the reactant concentration (0.01, 0.05, 0.1, 0.25, 0.5, 1.0 M) for fixed temperature and pressure similar to the conditions of product 11 in Table 1, and in Fig. 6 we show the corresponding PXRD data on the synthesis products. In this synthesis run, we have also controlled the temperature of the reaction block to 300 °C (Fig. 1). As before single phase anatase is obtained and in Fig. 7 the volume-averaged particle sizes obtained with PXRD are plotted. The particle size increases with increasing reactant concentration from 11 to 14 nm. Decreasing the reactant concentration below 0.01 M presumably will lead to a further decrease in particle size, but the mass of the synthesis product then decreases very sharply as well. This is an important parameter in an industrial process. On the other hand, it is clear that 14 nm particles can be produced even at high reactant concentrations making large-scale production possible. In the present set-up, a flow of 10 mL/min of a 0.1 M precursor meeting a 10 mL/min stream of supercritical solvent gives a yield of about 5 g/h. In an industrial application scaling up is simple, e.g., compared with scaling up a batch synthesis. One may note that the particles obtained with 0.1 M reactant and temperature-controlled reaction block are slightly larger than the particles obtained without temperature control of the reactant block (12.6 versus 11.3 nm). As seen in Table 1, a slight temperature drop in the overheated solvent due to lack of temperature regulation of the block was expected to have exactly this effect on the particle size.

### 3.2. Conventional sol–gel synthesis

In Table 2, we list particle size estimates obtained by SAXS for the conventional sol–gel synthesis products, and in Fig. 8 the particle diameters and heights are plotted as a function of synthesis time. PXRD data show that all

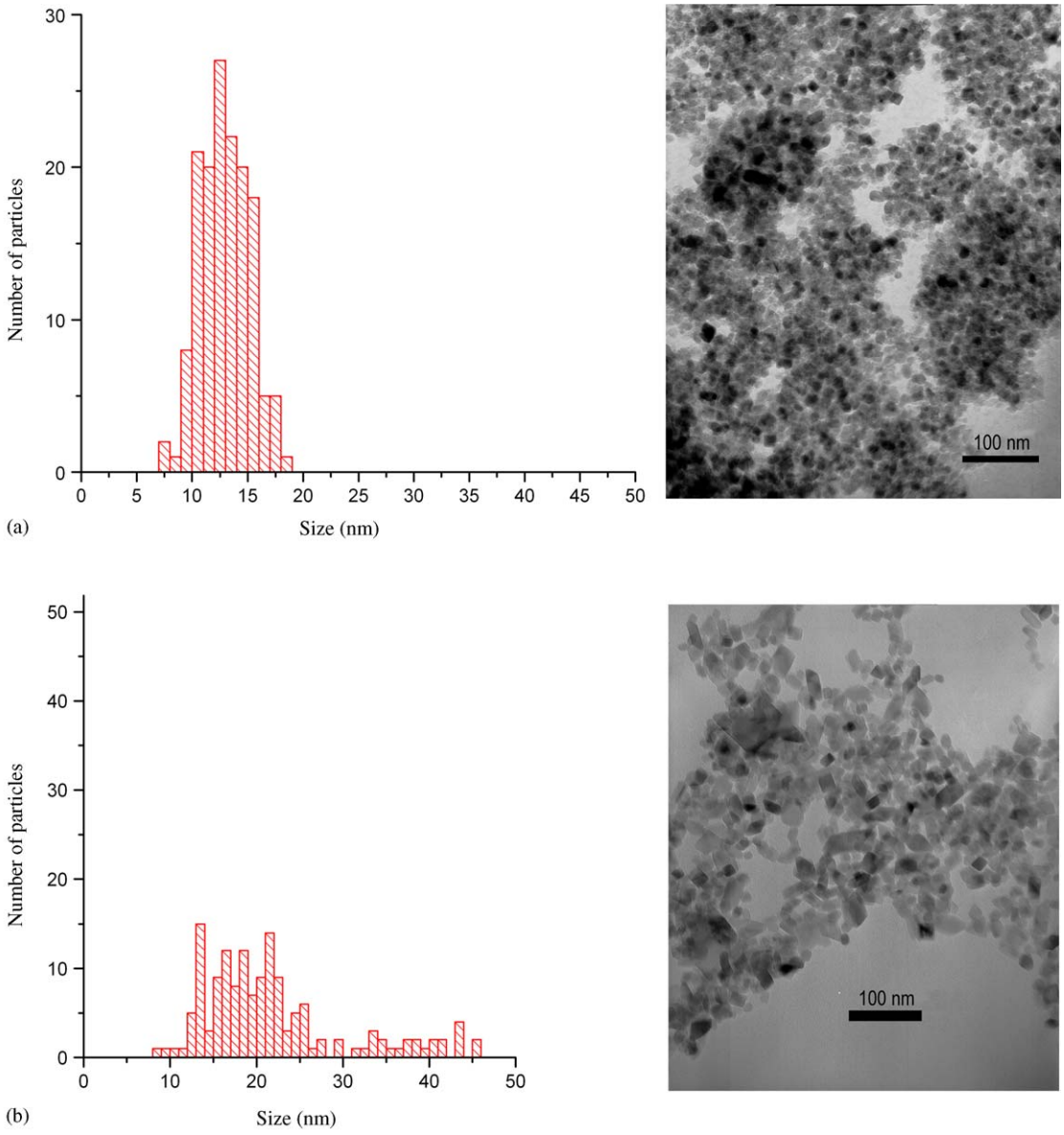


Fig. 4. (a) TEM image of product 11. The size distribution was derived from 150 particles in the image giving $13 \pm 2$ nm.(b) TEM image of a product synthesised by a conventional sol–gel method at 250 °C for 24 h. The size distribution was derived from 150 particles in the image giving $22 \pm 8$ nm.

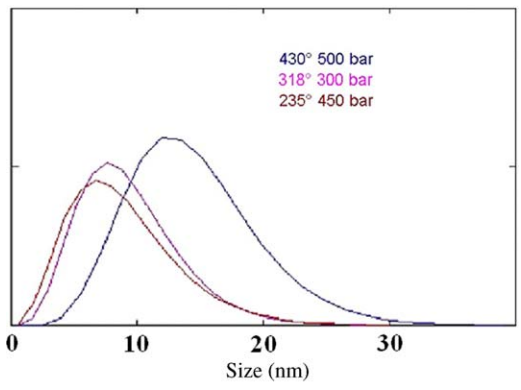


Fig. 5. Particle size distributions for supercritical synthesis products 8, 11 and 13 obtained from the SAXS data.

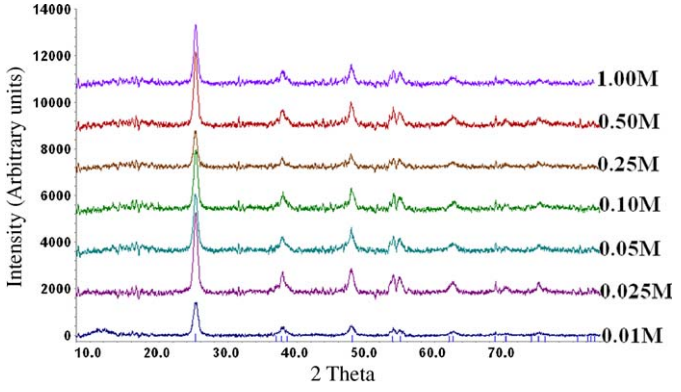


Fig. 6. Powder X-ray diffraction data from supercritical synthesis products obtained with variable reactant concentration and T = 300 °C, P = 300 bar.

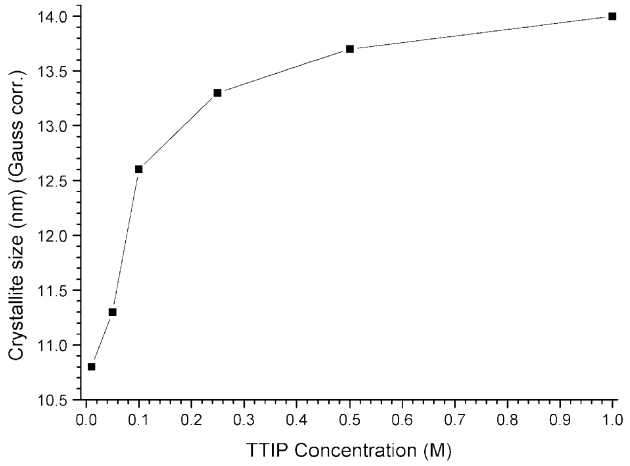


Fig. 7. Particle size (PXRD) as a function of reactant concentration for supercritical synthesis with $P = 300$ bar and $T = 300\,^{\circ}C$.

Table 2
Experimental details for the 15 synthesis products obtained with conventional sol–gel synthesis

| | $^1/_2$ h | 1 h | $1^1/_2$ h | 2 h | 24 h |
|---|---|---|---|---|---|
| 150 °C | 8.9 | 6.6 | 6.4 | 5.8 | 10.3 |
| | 3.7 | 3.8 | 4.4 | 4.6 | 1.7 |
| 200 °C | 11.2 | 13.7 | 15.1 | 13.3 | 17.2 |
| | 6.9 | 9.7 | 10.7 | 10.7 | 13.1 |
| 250 °C | 12.5 | 16.8 | 17.4 | 17.9 | 21.8 |
| | 9.4 | 11.1 | 11.9 | 12.3 | 17.4 |

Size characterisation was done with SAXS. The first entry is the disk diameter and the second entry the disk height [13].

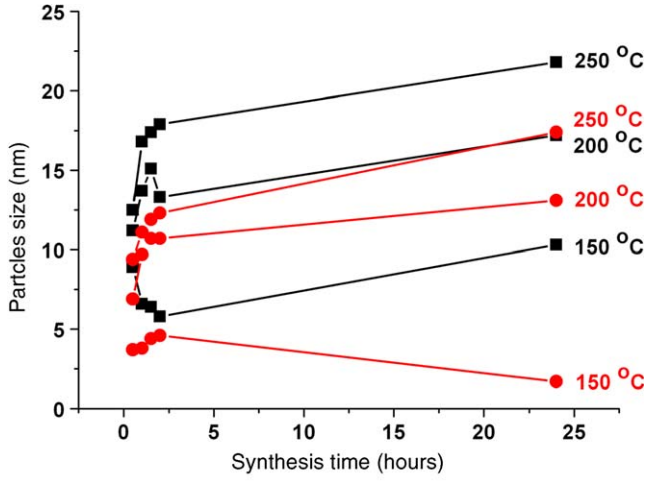


Fig. 8. Particle size (SAXS) as a function of synthesis time for the conventional sol–gel process. The squares refer to particle diameter (black), and the circles to particle height (red).

products are phase-pure anatase (data not shown). Fig. 8 nicely demonstrates that increasing synthesis time or temperature leads to an increase in both particle diameter and height. The only anomaly is the 150 °C/24 h synthesis, which shows a drop in disk height relative to shorter reaction times. As mentioned above, the TEM data on the sol–gel product show much broader size distributions than for the supercritical synthesis method. The agreement between TEM and SAXS size estimates for the 250 °C/24 h sol–gel synthesis product is excellent (22 nm for TEM, Fig. 4b; 21.8 nm for SAXS).

## 4. Conclusion

It has been demonstrated that highly homogenous and phase-pure anatase nanoparticles can be produced in seconds using a supercritical synthesis system. The tunability of supercritical fluids makes it possible to manipulate the size and size distribution of nanoparticles, thus removing one of the key limitations in application of nanomaterials. The small particle size and narrow size distribution is obtained because formation of a large number of primary particles is instantaneous when the hot supercritical solvent meets the cold reactant. The system described here is comparatively cheap, and pressure, temperature, flow rate and reactant concentrations can be changed continuously. Thus, the synthesis parameter space can quickly be mapped for a new reaction making optimisation straightforward. For all synthesis runs the size estimates obtained from PXRD, SAXS and TEM agree very well with typical particle sizes of $12 \pm 2$ nm at the low and intermediate supercritical temperature and pressure. The size increases to about 18 nm at high temperature ($>400\,^{\circ}C$) and high pressure ($>400$ bar). The excellent agreement between particle size estimates (SAXS, TEM) and crystallite size estimates (PXRD) suggests that the nanoparticles are highly crystalline even at synthesis times of the order of tens of seconds. For comparison, a series of conventional sol–gel syntheses were carried out. Single-phase anatase nanoparticles are also produced with this method, but the size distributions are much broader and the synthesis times are much longer.

## References

[1] M. Wilson, K. Kannangara, G. Smith, M. Simmons, B. Raguse, Nanotechnology, Basic Science and Emerging Technologies, CRC Press, Boca Raton FL, 2002.
[2] (a) H.S. Nalwa, Nanoclusters and nanocrystals, American Scientific Publishers, Stevensons Ranch, 2003;
(b) K.J. Klabunde, Nanoscale materials in chemistry, Wiley, New York, 2001.
[3] (a) P.S. Shah, T. Hanrath, K.P. Johnston, B.A. Korgel, J. Phys. Chem. 108 (2004) 9574–9587;
(b) X. Ye, C.M. Wai, J. Chem. Ed. 80 (2003) 198–204;
(c) Y. Arai, T. Sako, Y. Takebayashi, Supercritical Fluids, Molecular Interactions, Physical Properties and New Applications, Springer, Berlin, 2002;
(d) H. Weingärtner, E.U. Franck, Angew. Chem. Int. Ed. 44 (2005) 2672–2692.
[4] (a) J.A. Darr, M. Poliakoff, Chem. Rev. 99 (1999) 495–541;
(b) T. Sato, S. Kurosawa, R.L. Smith, T. Adschiri, K. Arai, J. Supercrit. Fluids 29 (2004) 113–119.

[5] (a) See for example the following references and references therein;
(b) T. Adschiri, K. Arai, in: Supercritical Fluid Technology in Materials Science and Engineering, Y. Sun, (Ed.), Marcel Dekker, New York, 2002, pp. 311–326;
(c) Y. Kakuta, T. Haganuma, K. Sue, T. Adschiri, K. Arai, Materials Research Bulletin 38 (2003) 1257–1265;
(d) A. Cabanas, M. Poliakoff, J. Mater. Chem. 11 (2001) 1408–1416.
[6] H. Jensen, K.D. Joensen, S.B. Iversen, E.G. Søgaard, Ind. Eng. Chem. Res. 45 (2006) 3348–3353.
[7] (a) J. Yu, X. Zhao, J. Du, W. Chen, J. Sol-Gel Sc. Technol. 17 (2000) 163–171;
(b) X.T. Zhang, O. Sato, M. Taguchi, Y. Einaga, T. Murakami, A. Fujishima, Chem. Mater. 17 (2005) 696–700.
[8] Y.V. Kolen'ko, A.A. Burukhin, B.R. Churagulov, N.N. Oleynikov, Mater. Lett. 57 (2003) 1124–1129.
[9] B.E. Warren, X-Ray Diffraction, Dover Publications, New York, 1990.
[10] A. Guinier, X-Ray diffraction in Crystals, Imperfect Crystals and Amorphous Bodies, Dover Publications, New York, 1994.
[11] J.S. Pedersen, J. Appl. Crystallogr. 37 (2004) 369–380.
[12] J.S. Pedersen, Adv. Colloid Interface Sci. 70 (1997) 171–210.
[13] J.S. Pedersen, in: P. Lindner, T. Zemb (Ed.), Neutron, X-rays and Light: Scattering methods Applied to Soft Condensed Matter, North Holland, 2002, Amsterdam, pp. 391–420.
[14] A. Weibel, R. Bouchet, F. Boulc'h, P. Knauth, Chem. Mater. 17 (2005) 2378–2385.
[15] J.I. Langford, D. Louër, Rep. Prog. Phys. 59 (1996) 131–234.